Anal. Chem. **2006,** *78,* 8281−8289

Field-Deployable, High-Resolution, Time-of-Flight Aerosol Mass Spectrometer

Peter F. DeCarlo,[†,‡] Joel R. Kimmel,[†] Achim Trimborn,[⊥] Megan J. Northway,[⊥] John T. Jayne,[⊥] Allison C. Aiken,[†,§] Marc Gonin,[∥] Katrin Fuhrer,[∥] Thomas Horvath,[∥] Kenneth S. Docherty,[†] Doug R. Worsnop,[⊥] and Jose L. Jimenez*[,†,§]

Cooperative Institute for Research in the Environmental Sciences (CIRES), University of Colorado, Boulder, Colorado 80309-0216, Department of Atmospheric and Oceanic Science, University of Colorado, Boulder, Colorado 80309-0311, Department of Chemistry and Biochemistry, University of Colorado, Boulder, Colorado 80309-0215, Aerodyne Research Incorporated, Billerica, Massachusetts 01821, and Tofwerk AG, Thun, Switzerland

The development of a new high-resolution time-of-flight aerosol mass spectrometer (HR-ToF-AMS) is reported. The high-resolution capabilities of this instrument allow the direct separation of most ions from inorganic and organic species at the same nominal *m/z*, the quantification of several types of organic fragments (C_xH_y, $C_xH_yO_z$, $C_xH_yN_p$, $C_xH_yO_zN_p$), and the direct identification of organic nitrogen and organosulfur content. This real-time instrument is field-deployable, and its high time resolution (0.5 Hz has been demonstrated) makes it well-suited for studies in which time resolution is critical, such as aircraft studies. The instrument has two ion optical modes: a single-reflection configuration offers higher sensitivity and lower resolving power (up to ∼2100 at *m/z* 200), and a two-reflectron configuration yields higher resolving power (up to ∼4300 at *m/z* 200) with lower sensitivity. The instrument also allows the determination of the size distributions of all ions. One-minute detection limits for submicrometer aerosol are <0.04 μg m^{-3} for all species in the high-sensitivity mode and <0.4 μg m^{-3} in the high-resolution mode. Examples of ambient aerosol data are presented from the SOAR-1 study in Riverside, CA, in which the spectra of ambient organic species are dominated by C_xH_y and $C_xH_yO_z$ fragments, and different organic and inorganic fragments at the same nominal *m/z* show different size distributions. Data are also presented from the MIRAGE C-130 aircraft study near Mexico City, showing high correlation with independent measurements of surrogate aerosol mass concentration.

Aerosols (small particles suspended in air) are ubiquitous in the atmosphere. They have adverse effects on human health[1] and play major roles in regional visibility degradation;[2] deposition of acids, toxins, and nutrients into ecosystems;[3] and the Earth's radiative balance (climate) and hydrological cycle.[4] Aerosols are also used in material manufacturing, nanotechnology, and pharmaceutical drug delivery.[5] The properties and effects of aerosols are strongly dependent on one extensive property, concentration, and three intensive properties: size, chemical composition, and shape (or morphology). The measurement of these properties in real time is difficult due to the inherent complexity of aerosols, their low mass concentrations (typically a few micrograms per cubic meter), and the large variability of their properties in space and time.

Over the last 15 years, mass spectrometry has emerged as a powerful tool to characterize aerosols. A number of laser ablation instruments have been developed. These instruments typically use optical signals in a particle flight chamber to aerodynamically size the particles and trigger a laser ablation time-of-flight mass spectrometer, which determines the composition of the sized particles.[6,7] A second type of aerosol instrument is based on thermal vaporization by contact with a heated surface rather than by ablation lasers.[8−10] At present, the most commonly used instrument of this type is the quadrupole-based Aerodyne aerosol mass spectrometer (Q-AMS), which uses flash thermal vaporization under high vacuum followed by electron impact ionization (EI) and mass analysis by a quadrupole mass spectrometer.[9,11,12] The advantages of this instrument include a particle size range

* Corresponding author. E-mail: jose.jimenez@colorado.edu.
† CIRES.
‡ Department of Atmospheric and Oceanic Science, University of Colorado.
§ Department of Chemistry and Biochemistry, University of Colorado.
⊥ Aerodyne Research Incorporated.
∥ Tofwerk AG.

(1) Dockery, D. W.; Pope, C. A.; Xu, X. P.; Spengler, J. D.; Ware, J. H.; Fay, M. E.; Ferris, B. G.; Speizer, F. E. *N. Engl. J. Med.* **1993**, *329*, 1753−1759.
(2) Watson, J. G. *J. Air Waste Manage. Assoc.* **2002**, *52*, 628−713.
(3) Likens, G. E.; Driscoll, C. T.; Buso, D. C. *Science* **1996**, *272*, 244−246.
(4) IPCC. *Intergovernmental Panel on Climate Change, Climate Change 2001: The Scientific Basis*; Cambridge University Press: Cambridge, England, 2001.
(5) Edwards, D. A.; Hanes, J.; Caponetti, G.; Hrkach, J.; BenJebria, A.; Eskew, M. L.; Mintzes, J.; Deaver, D.; Lotan, N.; Langer, R. *Science* **1997**, *276*, 1868−1871.
(6) Suess, D. T.; Prather, K. A. *Chem. Rev.* **1999**, *99*, 3007−3035.
(7) Murphy, D. M. *Mass Spectrom. Rev.* **2006**, in press.
(8) Tobias, H. J.; Kooiman, P. M.; Docherty, K. S.; Ziemann, P. J. *Aerosol Sci. Technol.* **2000**, *33*, 170−190.
(9) Jayne, J. T.; Leard, D. C.; Zhang, X. F.; Davidovits, P.; Smith, K. A.; Kolb, C. E.; Worsnop, D. R. *Aerosol Sci. Technol.* **2000**, *33*, 49−70.
(10) Voisin, D.; Smith, J. N.; Sakurai, H.; McMurry, P. H.; Eisele, F. L. *Aerosol Sci. Technol.* **2003**, *37*, 471−475.
(11) Canagaratna, M. R.; Jayne, J. T.; Onasch, T. B.; Williams, L. R.; Trimborn, A. M.; Northway, M. J.; Kolb, C. E.; Worsnop, D. R.; Jimenez, J. L.; Allan, J. D.; Coe, H.; Alfarra, M. R.; Zhang, Q.; Drewnick, F.; Middlebrook, A. M.; Delia, A.; Davidovits, P. *Mass Spectrom. Rev.* **2006**, in press.
(12) Jimenez, J. L.; Jayne, J. T.; Shi, Q.; Kolb, C. E.; Worsnop, D. R.; Yourshaw, I.; Seinfeld, J. H.; Flagan, R. C.; Zhang, X. F.; Smith, K. A.; Morris, J. W.; Davidovits, P. *J. Geophys. Res. [Atmos.]* **2003**, *108*, 8425; doi: 8410.1029/2001JD001213.

10.1021/ac061249n CCC: $33.50
Published on Web 11/11/2006

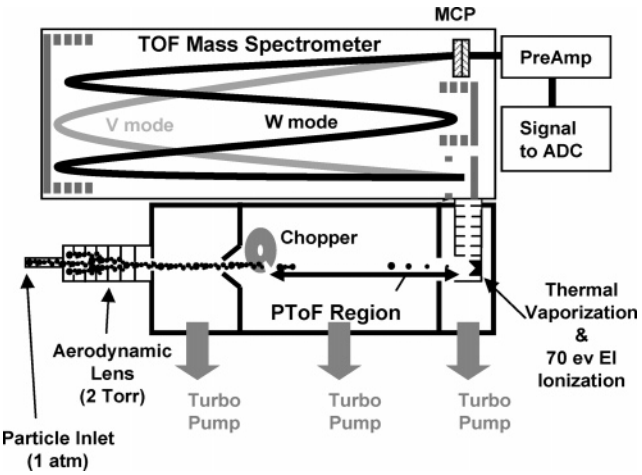

Figure 1. Schematic of the HR-ToF-AMS showing its two ion optical modes.

extending down to 35 nm by use of signal integration[13] and quantification of all species that are vaporized in a few seconds at a temperature of 600 °C (operationally defined as "nonrefractory", NR). Quantification is possible due to the universal and reproducible nature of EI as an ionization technique, the similar (and quantifiable) efficiency for all non-refractory species,[12] and the absence of matrix effects. In particular, ion−molecule reactions are avoided due to gas-phase ionization under high-vacuum conditions. A fraction of the particles containing less volatile species, such as ammonium sulfate, are known to bounce off the vaporizer and usually do this with a reproducible "collection efficiency", which adds some uncertainty to quantitation of ambient data.[14] A recent improvement of the AMS replaces the quadrupole mass analyzer with a compact time-of-flight mass spectrometer (C-ToF-AMS).[15] Although the C-ToF-AMS has better than unit mass resolution, this resolution is not generally sufficient to separate ions of different elemental composition at a nominal m/z.

This paper describes a new version of the AMS in which a high-resolution time-of-flight mass spectrometer has been adapted to the AMS (HR-ToF-AMS). The HR-ToF-AMS is the first real-time, field-deployable, aerosol mass spectrometer that is capable of directly distinguishing the elemental composition of ions having the same nominal mass. The next sections describe the instrument design and the evaluation of the instrument resolution and mass accuracy and present examples of the first high-resolution, ambient aerosol data obtained during the Study of Organic Aerosols in Riverside-1 (SOAR-1) and Megacities Impact on the Regional and Global Environment (MIRAGE) field campaigns.

EXPERIMENTAL METHODS

A schematic of the HR-ToF-AMS is shown in Figure 1. The sample introduction system, sizing region, and vaporization and ionization systems are of the same design as in previous versions of the AMS[9,15] and are only briefly summarized here. Ambient air is sampled through a critical orifice into an aerodynamic lens, which focuses particles ranging from ~35 nm to 1.5 μm in size into a narrow beam.[16] A supersonic expansion at the exit of the lens accelerates the particles into the sizing region (10^{-5} Torr), where particle size is determined by measuring flight time across a fixed distance. Time zero of particle flight is defined by a rotating mechanical chopper, and the end of particle flight is defined as the time of mass spectrometric detection. Particles are vaporized by impaction on a resistively heated surface (~600 °C) and ionized by electron ionization (70 eV). Only NR species are vaporized and detected; in practice, organic species and most nitrate and sulfate salts are detected, whereas crustal material, sea salt, and black carbon are not.

The generated ions have an initial distribution of energies related to the heat of vaporization (600 °C, $3kT/2 = 0.1$ eV). DC transfer optics between the source and the mass spectrometer are tuned to create a narrowly collimated beam within the TOFMS extractor. The energy distribution of this beam is determined primarily by the field used to extract ions from to ionization chamber. A strong extraction field leads to a higher ion transmission efficiency at the cost of an increased energy distribution (up to 20 eV). A slit just prior to the TOFMS extractor eliminates ions having excessive velocity components in the orthogonal direction (i.e., the TOFMS axis). Ions are extracted orthogonally[17] toward the reflectron, enabling efficient detection of the continuous ion beam.[18] The reflectron configuration maximizes flight path while maintaining a field-portable footprint.

This new version of the AMS uses a custom-designed Tofwerk AG (H-TOF Platform, Thun, Switzerland) high-resolution, orthogonal time-of-flight mass spectrometer. As shown in Figure 1, the HR-ToF-AMS includes ion optics for two modes of operation, referred to as V- and W-modes. V-mode is a standard reflectron-TOFMS configuration in which ions follow a trajectory from the extraction region into the reflectron and back to the multichannel plate (MCP) detector (effective ion path length $L = 1.3$ m). In W-mode, ions exiting the reflectron are directed into a hard mirror,[19] which focuses them back into the reflectron for a second pass before traveling to the MCP detector ($L = 2.9$ m). Both configurations have longer ion flight paths than the TOFMS previously used with the AMS,[15] roughly 3 and 6 times longer for the V- and W-modes, respectively. For ions originating from a given source and accelerated by a fixed potential, the mass resolving power of a TOFMS will increase as the flight path is lengthened. At the same time, lateral broadening of the ions increases over a longer flight path and reduces the total signal as fewer ions strike the detector. Therefore, the V-mode is the more sensitive, but the W-mode offers higher mass resolution.

Custom software developed in Visual Basic.NET (VB 7.0, Microsoft Corp., Redmond, WA) is used to control instrument timing, data acquisition, real-time preprocessing, and display. The details of timing are described below. Typical extraction periods are 30 μs (33 kHz) in V-mode and 50 μs (17 kHz) in W-mode,

(13) Zhang, Q.; Stanier, C. O.; Canagaratna, M. R.; Jayne, J. T.; Worsnop, D. R.; Pandis, S. N.; Jimenez, J. L. *Environ. Sci. Technol.* **2004**, *38*, 4797−4809.
(14) Huffman, J. A.; Jayne, J. T.; Drewnick, F.; Aiken, A. C.; Onasch, T.; Worsnop, D. R.; Jimenez, J. L. *Aerosol Sci. Technol.* **2005**, *39*, 1143−1163.
(15) Drewnick, F.; Hings, S. S.; DeCarlo, P.; Jayne, J. T.; Gonin, M.; Fuhrer, K.; Weimer, S.; Jimenez, J. L.; Demerjian, K. L.; Borrmann, S.; Worsnop, D. R. *Aerosol Sci. Technol.* **2005**, *39*, 637−658.
(16) Zhang, X. F.; Smith, K. A.; Worsnop, D. R.; Jimenez, J.; Jayne, J. T.; Kolb, C. E.; Morris, J.; Davidovits, P. *Aerosol Sci. Technol.* **2004**, *38*, 619−638.
(17) Chernushevich, I. V.; Ens, W.; Standing, K. G. *Anal. Chem.* **1999**, *71*, 452a−461a.
(18) Guilhaus, M.; Selby, D.; Mlynski, V. *Mass Spectrom. Rev.* **2000**, *19*, 65−107.
(19) Hohl, M.; Wurz, P.; Scherer, S.; Altwegg, K.; Balsiger, H. *Int. J. Mass Spectrom.* **1999**, *188*, 189−197.

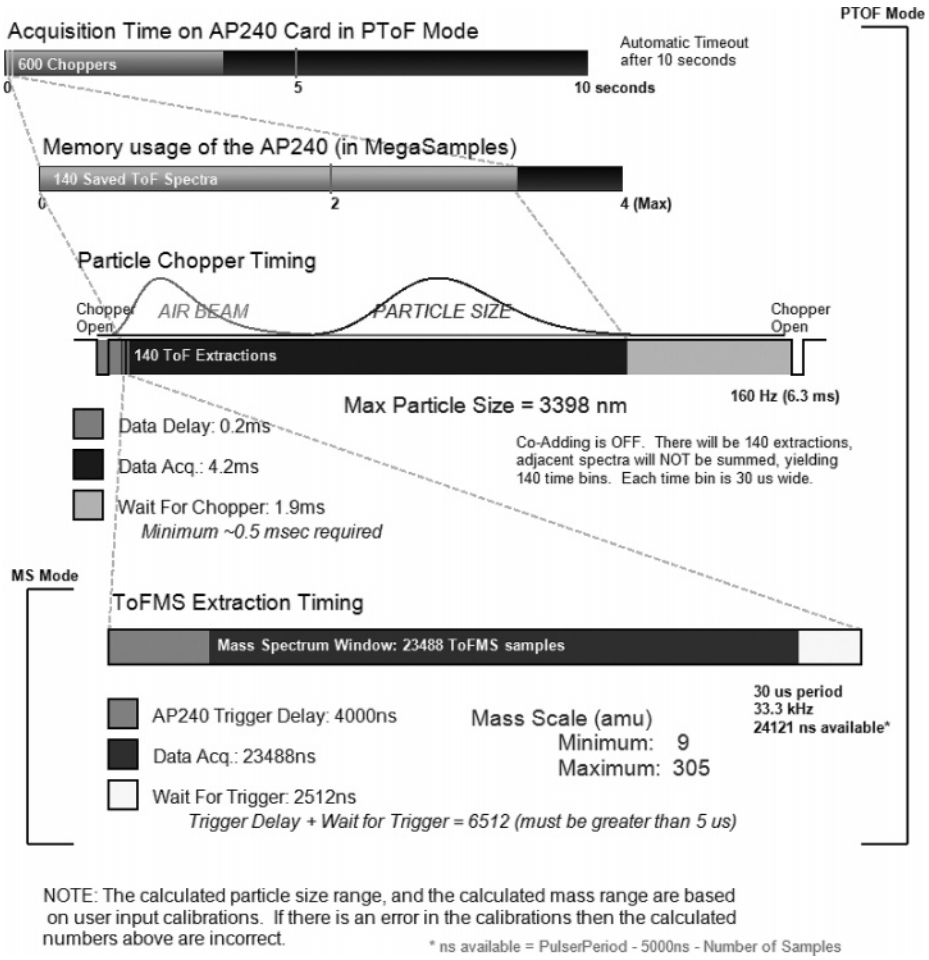

Figure 2. Timing diagram for use of the HR-ToF-AMS in PTOF mode (whole diagram) and MS mode (marked portion on bottom) showing allocations of AP240 board memory, time spent averaging on the board, particle size range for the timing settings, and *m*/*z* range for each of the extractions. Delays for the chopper and TOFMS extraction are required for timer card reset.

although other pulse rates can be used to span different *m*/*z* ranges. Signals from the MCP detector are amplified (55×) and sampled at 1 GHz with an 8-bit analog-to-digital converter (ADC) (AP240, Acqiris, Geneva, Switzerland). The ADC is equipped with digital thresholding, which detects ion pulses while rejecting electronic noise. Signal-to-noise ratios and dynamic range are maximized without rejection of small ion signals through a procedure that tracks the ratio of different gas-phase ion signals.[20]

Data flow for the instrument depends on the mode of operation.[12] In what is termed "mass spectrum (MS) mode," the particle beam is alternatively transmitted and blocked every ~3 s to allow the full particle and gas beam to pass into the instrument and to measure the background in the mass spectrometer, respectively. The full mass spectrum of the ensemble of all particles is recorded with no size information but with high duty cycle. A schematic of the timing scheme for this mode is shown at the bottom of Figure 2. In MS mode, ions are extracted at the pulsing rates described above. Spectra are co-averaged on the AP240 board with an 8-bit ADC, run with the "averager" firmware for the FPGA on-board processor. Data are typically transferred to PC RAM memory every few seconds, where they are further averaged for an amount of time specified by the user. This is generally on the order of tens of seconds to minutes, although data rates of ~0.5 Hz have been demonstrated.

In the sizing mode or "particle time-of-flight (PTOF) mode" (not to be confused with the ion time of flight in the mass spectrometer or ITOF), the timing of the instrument is considerably more complex. In this two-dimensional measurement, the mass spectrometer is used as a detector for particle time of flight. Particles exiting the aerodynamic lens have a size-dependent velocity. The particle beam is then pulsed by a mechanical chopper wheel rotating at ~160 Hz and with a slit opening of ~2%, initiating a "chopper cycle". The opening of the chopper slit defines the initial time (t_0) of the PTOF. After a delay on the order of 200 μs, the mass spectrometer acquires a set number of mass spectra separated in time by the extraction period (30 or 50 μs). The mass spectra are recorded sequentially in the board memory and sorted as a function of TOFMS extraction number since the chopper opening. This provides the mass spectra vs PTOF for a chopper cycle. Several hundred chopper cycles (~3 s) are typically averaged on the board memory by using the "round-robin" feature of the AP240 averager firmware. Adjacent mass spectra for each chopper cycle can be "co-added" on the board, which reduces data size at the expense of PTOF time (size) resolution. The

(20) Kimmel, J. R.; DeCarlo, P. F.; Worsnop, D. R.; Jimenez, J. L. Proceedings of the 54th American Society for Mass Spectrometry Conference, Seattle, Washington, October, 2006; http://cires.colorado.edu/jimenez-group/ToFAMSResources/ToFManual/Docs/Kimmel_ASMS_2006.pdf.

Table 1. Estimation of the Minimum Sampling Times for Representative Particle Counting Statistics for the Four Versions of the AMS

calculation inputs	quad	TOF
ambient no. concn (cm^{-3})	3000	
ambient "high mass particles" no. concn (cm^{-3})[a]	60	
flow rate (cm^{-3} s^{-1})	1.4	
chopper duty cycle in PTOF mode	2%	
chopper duty cycle in MS mode	50%	
duty cycle (due to peak shape) at each m/z	0.4	n/a
no. of m/z recorded in PTOF mode	10	300
no. of m/z recorded in MS mode	300	300
% of time in PTOF mode	50	50
data acquisition duty cycle	90%	90%
overall MS duty cycle per m/z	0.03%	22.5%
overall PTOF duty cycle per m/z	0.09%	0.90%
time to detect 10 particles at a given m/z in MS mode (s)	7.94	0.01
time to detect 10 "high mass" particles at a given m/z in MS mode (s)	397	0.53
time to detect 10 particles at a given m/z in PTOF mode (s)	2.65	0.26
time to detect 10 "high mass" particles at a given m/z in PTOF mode (s)	132	13.2

[a] It is typically observed for ambient particle distributions that a small fraction of the submicrometer particles contain most of the particle mass. For an approximate quantification of this effect on averaging times, we use a previous determination that 2% of the ambient particles contained ~50% of the particle mass for an ambient dataset in the Boston area.[12]

averaged chopper cycle data are transferred to computer memory, where they are processed, further averaged (typically from seconds to minutes), and saved to disk. The MS and PTOF modes are typically alternated every few seconds as part of the "general alternation mode" of the software. Table S-1 in the Supporting Information section shows characteristic timing setups for the two different instrument modes and for two different m/z ranges.

A third data acquisition mode, known as the "brute-force single-particle (BFSP) mode" has also been implemented. This mode can be alternated every few seconds with the MS and PTOF modes. The BFSP mode is a version of the PTOF mode in which a single chopper cycle is captured and transferred to computer memory without averaging multiple chopper cycles on the AP240 board. After transfer to computer memory, BFSP data may be filtered with user-defined, single-particle signal thresholds on multiple m/z's or combinations of m/z's, allowing the identification of single particle events[12] and recording full mass spectra of these events.[15] The main disadvantage of this mode, at present, is its low duty cycle (~3%) due to the high overhead for transferring large amounts of data from AP240 memory to computer memory through the PCI bus. Changes are being made to the acquisition software to improve this duty cycle through on-board data compression. Note that in BFSP mode some "blank cycles" are recorded, during which no particle arrived to the AMS vaporizer. For example, with the particle concentration and instrument characteristics in Table 1, we can estimate an average of 0.75 particles entering the instrument per chopper opening. Because there are 70−160 mass spectra recorded sequentially in this mode and a particle produces signals over 3−5 spectra, there will be many blank spectra in the data matrix.

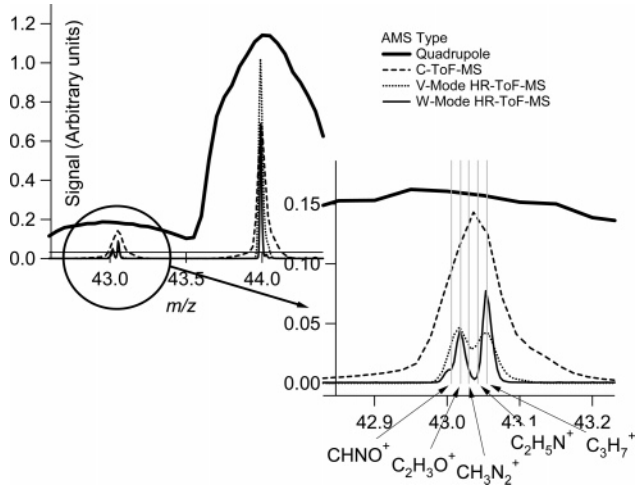

Figure 3. Peak comparisons for the four versions of the AMS. Resolution improvements are obvious in the progression from Q-AMS to C-ToF-AMS to V-mode to W-mode of the HR-ToF-AMS.

RESULTS AND DISCUSSION

Real-Time High-Resolution Data. The main benefit of the HR-ToF-AMS is its increased mass resolution. Figure 3 shows a comparison of the raw ion signals from ambient aerosols for the four AMS designs at m/z 43−44. The inset highlights the resolution for the TOF instruments at m/z 43. The Q-AMS and the C-ToF-AMS are unable to separate ions at this nominal mass. The V-mode data clearly show the ion signals of $C_2H_3O^+$ and $C_3H_7^+$, and the W-mode data, in addition to the first two ions, also show a third peak on the shoulder of the $C_2H_3O^+$ ion corresponding to $CHNO^+$. Other commonly used aerosol mass spectrometers have resolving powers from 100 to 1000 (personal communication, Murray Johnston, Kim Prather, Dan Murphy),[21,22] with the higher end of this range being slightly better than for the C-ToF-AMS resolution in Figure 3. Thus, due to its high resolving power, the HR-ToF-AMS is the first real-time aerosol mass spectrometer with the capability to separate different organic ions at the same nominal m/z.

Instrument Characterization. Shown in Figure S-1 of the Supporting Information are example mass spectra in V- and W-modes while sampling perfluorokerosene (PFK, Sigma-Aldrich) particles that were generated from a solution of PFK in isopropyl alcohol using a constant output atomizer (TSI model 3076, St. Paul, MN). The polydisperse particles were diffusion-dried and sampled with the HR-ToF-AMS. The approximate concentration of PFK entering the instrument was 1 mg m^{-3}. The insets show the detection of ion peaks up to m/z's 1340 and 680 in V- and W-mode, respectively. This is important for some species containing large, stable molecules, such as polycyclic aromatic hydrocarbons, which resist fragmentation in EI and are atmospherically relevant due to their high toxicity[23] and also for the use of this spectrometer with "soft-ionization" sources for the characterization of high-

(21) Erdmann, N.; Dell'Acqua, A.; Cavalli, P.; Gruning, C.; Omenetto, N.; Putaud, J. P.; Raes, F.; Van Dingenen, R. *Aerosol Sci. Technol.* **2005**, *39*, 377−393.
(22) Lake, D. A.; Tolocka, M. P.; Johnston, M. V.; Wexler, A. S. *Environ. Sci. Technol.* **2003**, *37*, 3268−3274.
(23) Dzepina, K.; Arey, J.; Marr, L. C.; Worsnop, D. R.; Salcedo, D.; Zhang, Q.; Molina, L. T.; Molina, M. J.; Jimenez, J. L. *Int. J. Mass Spectrom.* **2006**, submitted.

molecular-weight species and oligomers.[24] In addition, there is a sensitivity improvement at high m/z with respect to the C-ToF-AMS from the easier separation of ion peaks from the underlying baseline.

Two key characteristics of atmospheric instrumentation are high time resolution and low detection limits. In the AMS, time resolution is often limited by particle-counting statistics: unlike when analyzing for gas-phase species, analyte molecules arrive in discrete and infrequent packets (the particles) each typically containing millions to billions of molecules. This limits the shortest averaging time for meaningful concentration reporting for a given ambient particle loading to the time to sample a minimally representative number of particles. Bahreini et al.[25] showed that counting statistics limited the Q-AMS in MS mode to reporting times of ~1−5 min under typical ambient conditions, although much shorter averaging times are possible with this instrument when directly sampling high particle concentrations, such as at sources,[26] or using selected ion monitoring. In Table 1, the Q and TOF versions of the AMS are compared in terms of time required to sample 10 particles while running the instrument under typical rural tropospheric sampling conditions. Note that minimum averaging times will be shorter under polluted conditions due to the larger particle number concentrations. All ToF-AMSs can measure a minimally representative number of particles on the order of seconds. The reduction in required averaging time for the ToF-AMS instruments with respect to the Q-AMS is largest in MS mode (~×800). This advantage arises because the TOF instruments detect all m/z values simultaneously, whereas the quadrupole instrument scans across m/z values. The improvement is smaller in PTOF mode (~×10) because the Q-AMS only scanned selected ions in this mode. However, the PTOF mode data are much richer for the TOF instruments, which can measure size distributions for all m/z's versus a small subset for the Q-AMS.

Table 2 compares the measured detection limits (DLs) of the main AMS designs. DLs are defined in MS mode since the signal-to-noise ratio is highest in this mode. From the previous discussion, we would expect an improvement of $\sim\sqrt{800}$ (~28) for the ToF-AMSs over the Q-AMS due to the increased averaging time (duty cycle) at each m/z. Improvements of this order are, indeed, achieved with the C-ToF-AMS. The V-mode of the HR-ToF-AMS also produces large improvements versus the Q-AMS, and the W-mode DLs are similar to those of the Q-AMS. The differences among the three TOF versions are due to the differences in ion throughput for the three instruments. The final row in Table 2 is a comparison of the N_2^+ ion frequency ("airbeam", from ionization of the gas beam entering the instrument with the particle beam) as measured by all the AMS instruments. N_2^+ frequency is a good proxy for signal levels and illustrates the ion throughput in the different TOF based instruments. Since the sample introduction, vaporization, and ionization processes are the same across all versions of the ToF-AMS, the higher detection limits (lower signal)

Table 2. Measured 1-Min Detection Limits in MS Mode for the Four Versions of the AMS

	detection limits[a] (ng m^{-3})			
	HR-ToF-AMS			
	W-mode	V-mode	C-ToF-AMS	quadrupole[33]
organics	360	22	19	470
sulfate	110	5.2	2.2	160
nitrate	32	2.9	1.2	32
ammonium	150	38	16	350
chloride	53	12	4.0	32
N_2^+ ion (Hz)[b]	10^4	2.5×10^5	10^6	7×10^3 [b]

[a] Detection limits of different species were determined as 3× the standard deviation of mass concentrations for 1-min averages of filtered air. The quadrupole DL data was scaled to 1 min from 10 min as (1-min DL = 10-min DL × sqrt(10/1)). [b] By convention, the N_2^+ ion rate is the background-subtracted rate during the periods in which the chopper is in the open position. The N_2^+ ion rate reported here is the rate actually measured during MS mode. During operation, the Q-AMS data acquisition software reports this rate as if the instrument were performing single ion monitoring at m/z 28, which corresponds to a rate of 5×10^6 Hz.

in the V- and W-modes of the HR-ToF-AMS in comparison to the C-ToF-AMS are due to lower ion throughput in the instruments. In addition to the loss of signal due to lateral separation, as mentioned previously, some of the reduced throughput is due to the increased separation between the extraction region and the MCP in the V- and W-modes in comparison to the C-ToF-AMS. The square root of the ratio of the N_2^+ frequencies for different TOF instruments is approximately the factor difference in the detection limits of the instruments.

m/z Calibration. The HR-ToF-AMS has been designed as a field instrument that can operate continuously while unattended for days and even weeks. Thus, a robust procedure to perform automated mass calibration of the instrument without the use of external standards is needed. For this reason, the m/z scale is calibrated using known peaks in the instrument background spectra, which are highly reproducible in time and across instruments. Typical background peaks with little interference include C^+ (m/z 12), O^+ (16), O_2^+ (32), Ar^+ (40), $C_7H_7^+$ (91), $C_8H_5O_3^+$ from phthalates (149), and $^{184}W^+$. For each peak, the highest point and two points to either side are used. These five points are fitted to a Gaussian in ITOF space to obtain the position of the peak center. Using the ITOFs of the peak centers for several m/z and their known exact masses, the data are fit with the following power law to determine the relationship between ITOF and m/z.

$$t = a(m/z)^b + c \quad (1)$$

$$m/z = \left(\frac{t-c}{a}\right)^{1/b} \quad (2)$$

The values a, b, and c are determined by a Levenberg−Marquardt algorithm (Igor Pro Version 5, Wavemetrics, Lake Oswego, OR) fit to these data. The choice of the power law fit instead of forcing the parameter b to be 0.5 (as in the ideal square root relationship for TOF instruments) allows one extra degree of freedom in the mass calibration, and unlike a higher-order polynomial relationship, it can be extrapolated outside of the range of calibration

(24) Kalberer, M.; Paulsen, D.; Sax, M.; Steinbacher, M.; Dommen, J.; Prevot, A. S. H.; Fisseha, R.; Weingartner, E.; Frankevich, V.; Zenobi, R.; Baltensperger, U. *Science* **2004**, *303*, 1659−1662.

(25) Bahreini, R.; Jimenez, J. L.; Wang, J.; Flagan, R. C.; Seinfeld, J. H.; Jayne, J. T.; Worsnop, D. R. *J. Geophys. Res. [Atmos.]* **2003**, *108*, 8645; doi: 8610.1029/2002JD003226.

(26) Canagaratna, M. R.; Jayne, J. T.; Ghertner, D. A.; Herndon, S.; Shi, Q.; Jimenez, J. L.; Silva, P. J.; Williams, P.; Lanni, T.; Drewnick, F.; Demerjian, K. L.; Kolb, C. E.; Worsnop, D. R. *Aerosol Sci. Technol.* **2004**, *38*, 555−573.

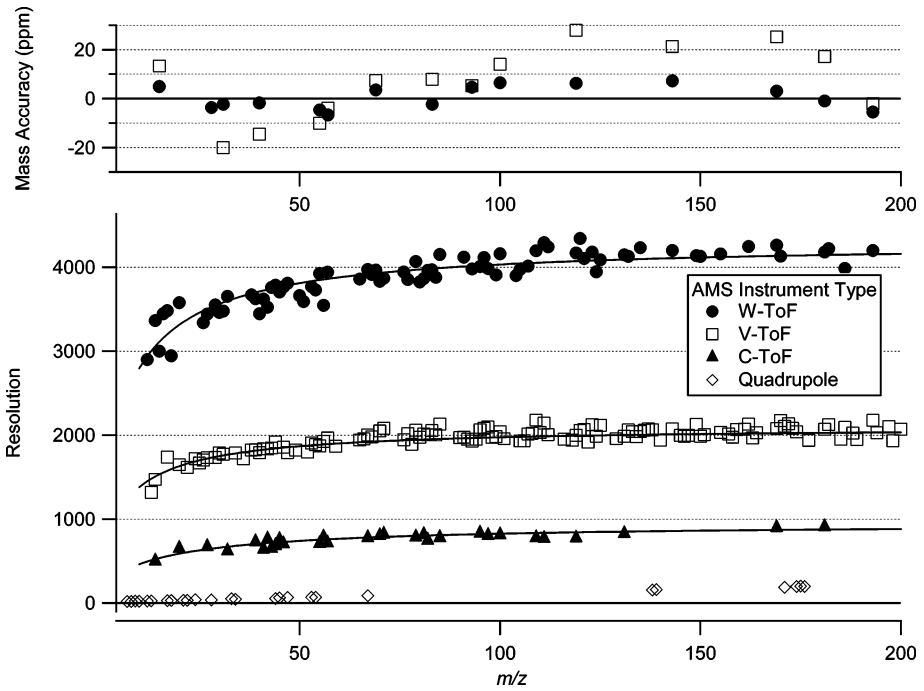

Figure 4. (a) Mass accuracy of the V- and W-modes of the HR-ToF-AMS vs *m*/*z*. (b) Resolution of the four AMS instrument types vs *m*/*z*. Lines through the resolution points are the sums in quadrature of the single ion width and the resolving power of the TOFMS. PFK and some selected low-mass ions were used as the analyte in both (a) and (b) after a typical *m*/*z* calibration was performed from the background spectrum (see text).

masses with reasonable accuracy. Slight variations on the value of *b* can arise from variations of the effect of the finite extraction pulse and region for different *m*/*z*.[18] Typically, the values of *b* returned by the fit are less than 1 ppt away from 0.5 (e.g., 0.499 951).

Mass Accuracy for Field Measurements. Using the *m*/*z* calibration based on background ions described above, a calculation of the mass accuracy of the instrument applicable to field data can be performed. Ion peaks with known exact *m*/*z*'s can be generated from PFK as described above. Using the ions arising from these particles as the sample (not as the calibrant), we can compare the *m*/*z* values determined with our calibration procedure with the known exact *m*/*z*'s. Figure 4a shows the results of this experiment. As can be seen, the mass accuracy of the W-mode with the background-based calibration is 7 ppm or better for the masses of interest. For V-mode data, this accuracy is 28 ppm or better. Note that when performing controlled lab experiments, PFK can be used as a calibrant during the acquisition of the data, which allows for the possibility of better mass accuracy with respect to the procedure described here for field data, given the systematic trends vs *m*/*z* observed in the accuracy graph.

Mass Resolving Power. The resolving power of the instrument is defined as $m/\Delta m$, with m being the nominal *m*/*z* and Δm being full-width at half-maximum (fwhm).[27] Figure 4b shows the measured resolution vs *m*/*z* for the main AMS designs. There is a clear progression toward higher resolution as Q-AMS < C-ToF-AMS < V-mode of HR-ToF-AMS < W-mode of HR-ToF-AMS. The highest resolutions for each instrument for the *m*/*z* range (10−200) shown are about 220, 800, 2100, and 4300, respectively. The lines through the data are generated by summing the fwhm of the single ion response in nanoseconds with the constant resolving power of the TOFMS in nanoseconds in quadrature. For the C-ToF-AMS, this yields values of 2 ns for the SI width and a maximum resolving power of 950. The SI width, as measured by a custom software algorithm,[20] for the V- and W-mode is 1.4 ns, with a maximum resolving power at *m*/*z* 200 of 2100 and 4300, respectively. Although much higher resolving powers have been achieved by many mass spectrometers, the W-mode values are the highest resolutions reported to date for a real-time field-deployable aerosol mass spectrometer. The W-mode resolution is also sufficient to separate most of the important ions for atmospheric aerosols observed so far, especially at *m*/*z* < 100 where most of the signal appears for the EI AMSs, as exemplified below. The resolution is reduced at smaller *m*/*z* due to the influence of the digitization time step of the ADC (1 ns) and of the finite width (~1.4 ns) of the MCP response to a single ion.

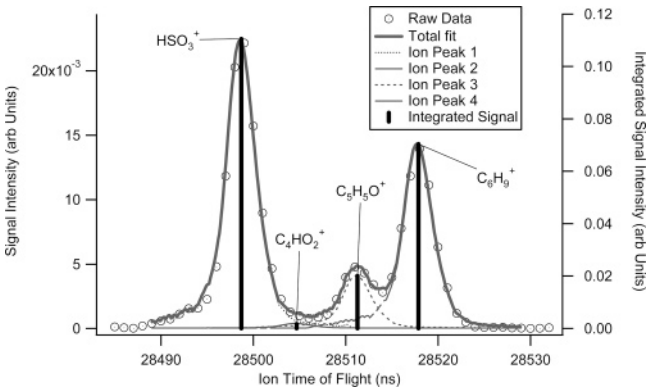

Figure 5. Results from fitting algorithm to obtain the signal of each individual ion for *m*/*z* 81.

(27) Cotter, R. J. *Time-of-Flight Mass Spectrometry: Instrumentation and Applications in Biological Research*; American Chemical Society: Washington, D.C., 1997.

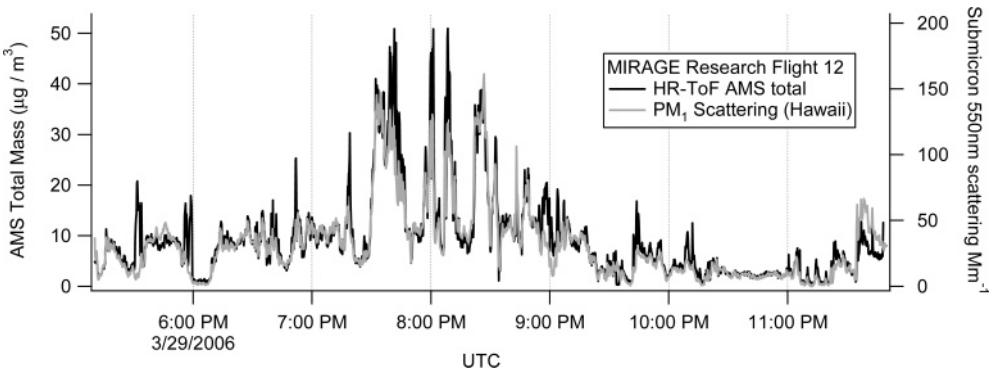

Figure 6. Comparison of the HR-ToF-AMS NR-PM_1 mass concentrations with the total PM_1 light scattering for research flight 12 of the NCAR C-130 aircraft during the MIRAGE field campaign.

The limiting widths due to these two effects have a larger proportional effect for these lower m/z's, whose intrinsic distributions of arrival times are sharper in a TOFMS.[28] The effect is more pronounced as the instrument resolution increases. Ongoing improvements in the data acquisition software aim to reduce or eliminate this effect.

Signal Integration for Ions of the Same Integer m/z. For quantification, the total ion current of each ion must be determined.[12] In a TOFMS, this corresponds to the signal area (not height) in the spectrum, the calculation of which is limited by overlapping peaks at the resolution levels achieved here. A custom peak-fitting routine has been developed to quantify the ion signal from overlapping ion peaks at each integer m/z. This algorithm uses an array of user-defined possible ions (exact m/z's). Each ion is represented with a custom peak shape function, which is the product of a Gaussian peak with a custom function,

$$P_i(t) = he^{(-((t-t_0)/\sigma)^2)} f\left(\frac{t-t_0}{\sigma}\right) \quad (3)$$

where $P_i(t)$ is the peak intensity for one ion as a function of ITOF (t), h is a peak intensity parameter, t_0 is the ITOF for the exact m/z of interest based on the m/z calibration, and σ is the Gaussian peak width. σ has a linear dependence on m/z for masses below 100, as shown in Figure S-2 of the Supporting Information for SOAR-1 data. $f((t-t_0)/\sigma)$ is a custom function for accounting for deviations from a purely Gaussian peak shape, derived before signal integration from known isolated ions in the background spectrum. Figure S-3 of the Supporting Information shows a peak shape function also for SOAR-1 data. This peak shape function is highly dependent on the detailed tuning of the TOFMS and can be highly variable away from the peak center. The ion current is determined as the area of the Gaussian multiplied by a scalar to account for the custom peak shape. The scalar is constant across all m/z. At each integer m/z, σ is assumed to be the same for all peaks, and the total signal is the linear combination of the signals of each individual ion,

$$P(t) = \sum_{i=0}^{n} P_i(t) \quad (4)$$

where $P(t)$ is the total signal for an integer m/z, and n is the number of ions considered at that m/z. The total signal with unit m/z resolution can be used with existing algorithms for processing Q-AMS data[29] to obtain a real-time estimate of species mass concentrations and the total organic fragmentation pattern.

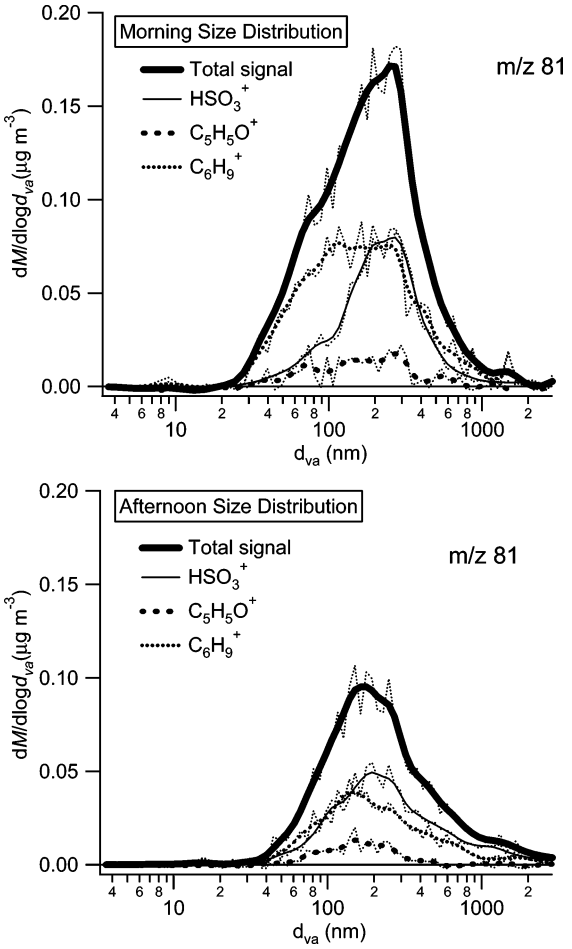

Figure 7. Size distributions of individual ions and total signal for m/z 81. Data from SOAR-1 field campaign in Riverside 2005, morning average from 7:30 to 8:30 on August 10, 2005, afternoon average from 13:50 to 14:50 on August 9, 2005.

(28) Guilhaus, M.; Mlynski, V.; Selby, D. *Rapid Commun. Mass Spectrom.* **1997**, *11*, 951−962.

(29) Allan, J. D.; Delia, A. E.; Coe, H.; Bower, K. N.; Alfarra, M. R.; Jimenez, J. L.; Middlebrook, A. M.; Drewnick, F.; Onasch, T. B.; Canagaratna, M. R.; Jayne, J. T.; Worsnopf, D. R. *J. Aerosol Sci.* **2004**, *35*, 909−922.

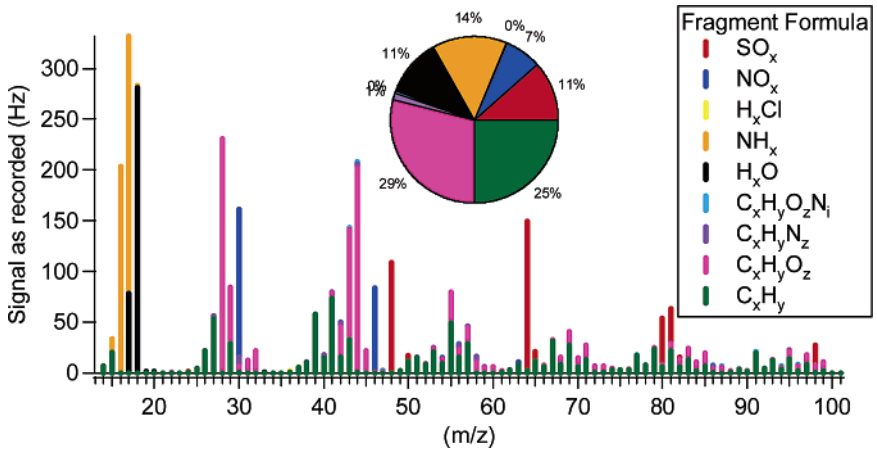

Figure 8. Composite mass spectrum showing the total recorded signal (ion duty cycle correction[15] has not been applied) at each *m*/*z* and the types of ions that contribute to those signals for 4−4:05 PM on August 8, 2005 during the SOAR-1 field study. A unit resolution mass spectrometer would only be able to determine total peak height for each of these *m*/*z*'s. Signal for $C_xH_yO_z$ at *m*/*z* 28 was estimated as 1.15 × CO_2^+ signal.[32,34] (1.15 was chosen as the average value found for the two studies cited.) The signal at *m*/*z* 18 is the total particle-phase signal and has not been partitioned into fraction from sulfate, organic, or particle water.[29]

Shown in Figure 5 is the application of the peak-fitting algorithm to *m*/*z* 81 data taken during the SOAR-1 field campaign (http://cires.colorado.edu/jimenez-group/Field/Riverside05/). There are three clearly distinguishable peaks, with a fourth peak in the tail of one of the larger signals. The small fourth peak is at the limit of what the algorithm can identify. For this fitting procedure to work, all important ions present must be included in the fitting procedure. Failure to include ions that are present in the sample can result in significant errors or lack of convergence. Thus, it is important to develop a list of *m*/*z*'s that are present with significant intensity for a given application (e.g., atmospheric aerosols). Although a large number of atomic combinations are chemically possible, in principle, for ions at many *m*/*z*'s, this problem is less severe for the lower *m*/*z*'s, where most of the signal is concentrated when using EI. In addition, many of the atomic combinations that are possible in principle are not present for the atmospheric aerosols observed so far, either due to the refractory nature of their aerosol species (e.g., soil dust or refractory oxides, although metals can and have been detected, but this is dependent on their chemical state) or to the low concentration of the compounds in the aerosol (e.g., compounds containing B or P). A list of ions applicable to atmospheric aerosols is being developed and will be presented in a future publication.

Very High Time Resolution. The use of the instrument in V-mode allows for fast acquisition of ambient data with excellent detection limits. During the MIRAGE field campaign (http://mirage-mex.acd.ucar.edu/) the HR-ToF-AMS was deployed on the National Center for Atmospheric Research (NCAR) C-130 aircraft and sampled the pollution plume over and downwind of Mexico City. The instrument was run in V-mode to maximize sensitivity, and data were recorded every 12 s. Figure 6 shows a comparison between the total measured mass by the HR-ToF-AMS and submicrometer light-scattering at 550 nm measured by the University of Hawaii with a TSI nephelometer (10-s resolution). Scattering is often used as a surrogate of particle mass concentration, but it is a fundamentally different measurement. The high degree of correlation as particle concentrations increase and decrease during the flights highlights the high time resolution and the quantitative ability of the HR-ToF-AMS.

Size-Resolved Chemistry. We conclude by presenting two examples of ambient aerosol data acquired with the W-mode during the SOAR-1 field campaign. Figure 7 shows the signal for the three different ions that contribute to nominal mass 81 versus vacuum aerodynamic diameter (d_{va})[30] for morning and afternoon averages. Solid lines are the result of three-point binomial smoothing applied to the raw data. An aerosol concentrator[31] was used to enhance the particle concentration by a factor of ~12 and allow higher time resolution during this experiment. Also shown is the sum of all the different *m*/*z* 81 ions, which represent the size distribution that the unit-mass resolution versions of the AMS (Q-AMS and C-ToF-AMS) would report. The size-resolved chemistry changes significantly during the day. In particular, during the morning rush hour, the $C_6H_9^+$ fragment is dominant for smaller particles. This is likely due to traffic emission particles' being more abundant in the morning, many of which are fractal in nature and appear at small d_{va} in the AMS,[30] and whose NR composition is dominated by hydrocarbons.[26] The sulfate fragment is in the size typical of accumulation mode particles for the morning sample, shifting to lower average sizes due to a reduction of its accumulation mode concentration in the afternoon.

Separation of Ion Fragment Groups. The ability to quantitatively separate the signal from different ions at each nominal *m*/*z* allows for new ways to organize and classify data. Shown in Figure 8 is one way to present the increased chemical information content of the HR-ToF-AMS, using one 5-min average spectrum from the SOAR-1 study (4−4:05 PM 8/8/2005). Ions are separated into different inorganic and organic fragment classes on the basis of the atoms contained in each ion. A unit resolution mass spectrometer would only be able to determine the total height of the peaks; it would be unable to directly classify the signal into these different ion classes. Note that the C_xH_y and $C_xH_yO_z$ ion classes do not directly correspond to the hydrocarbon-like organic aerosol (HOA) and oxygenated organic aerosol (OOA) compo-

(30) DeCarlo, P.; Slowik, J.; Worsnop, D. R.; Davidovits, P.; Jimenez, J. *Aerosol Sci. Technol.* **2004**, *38*, 1185−1205; doi: 1110.1080/027868290903907.

(31) Khlystov, A.; Zhang, Q.; Jimenez, J. L.; Stanier, C.; Pandis, S. N.; Canagaratna, M. R.; Fine, P.; Misra, C.; Sioutas, C. *J. Aerosol Sci.* **2005**, *36*, 866−880.

nents identified by Zhang et al.[32] Although these ion classes and time series components are related, on the basis of source-sampling experiments, HOA does contain some $C_xH_yO_z$ ions, and OOA does contain some C_xH_y ions. The pie chart in Figure 8 shows the relative contribution of each ion class to the total aerosol mass. Future work will apply principal component analysis techniques[32] to time series of this type of data to gain insight into the complex chemistry of the atmospheric aerosol.

CONCLUSIONS

The AMS allows for the quantitative measurement of size-resolved chemistry of submicrometer nonrefractory aerosol with high time resolution and high sensitivity. The HR-ToF-AMS retains these characteristics while allowing an improved chemical characterization of the aerosol. This is due to its quantification of the signal from ions of different atomic compositions, a unique ability for a real-time aerosol field instrument. Resolving powers of 2100 and 4300 and mass accuracies of ±28 and ±7 ppm (up to m/z 200) have been demonstrated for the V-and W-modes of the HR-ToF-AMS, respectively. A signal area integration procedure has been demonstrated. Examples of HR-ToF-AMS data from recent field campaigns have been used to demonstrate the high time resolution and increased chemical and microphysicochemical resolution of the instrument.

(32) Zhang, Q.; Alfarra, M. R.; Worsnop, D. R.; Allan, J. D.; Coe, H.; Canagaratna, M. R.; Jimenez, J. L. *Environ. Sci. Technol.* **2005**, *39*, 4938−4952; doi: 4910.1021/es0485681.
(33) Zhang, Q.; Canagaratna, M. R.; Jayne, J. T.; Worsnop, D. R.; Jimenez, J. L. *J. Geophys. Res. [Atmos.]* **2005**, *110*, D07S09; doi: 10.1029/2004JD004649.
(34) Takegawa, N.; Miyakawa, T.; Kawamura, K.; Kondo, Y. *Aerosol Sci. Technol.* **2006**, submitted.

ACKNOWLEDGMENT

The authors thank A. Clarke, J. Zhou, Y. Shinozuka, and S. Howell from the University of Hawaii for the use of their Nephelometer data and C. Sioutas, P. Fine, M. Geller, and S. Sardar of the University of Southern California for the use of their aerosol concentrator. The authors also acknowledge funding from grants NSF CAREER ATM-0449815, NASA NNG04GA67G, and NSF/UCAR S05-39607 for funding the HR-ToF-AMS acquisition and/or development, and grants EPA RD-83216101-0 and NSF ATM-0513116 for supporting the SOAR and MIRAGE field studies, respectively. P.F.D. is grateful for an EPA STAR Fellowship (91650801). Any opinions, findings, and conclusions or recommendations expressed in this material are those of the authors and do not reflect the views of the funding agencies. We also thank P. Ziemann for his efforts in organizing the SOAR-1 field campaign, as well as Ed Dunlea for his help during Mirage, the rest of the Jimenez Group, and the rest of the AMS community for many useful discussions.

SUPPORTING INFORMATION AVAILABLE

Additional information as noted in text. This material is available free of charge via the Internet at http://pubs.acs.org.

Received for review July 10, 2006. Accepted September 11, 2006.

AC061249N

Supplementary Information

A Field-Deployable High-Resolution Time-of-Flight Aerosol Mass Spectrometer

P. F. DeCarlo[1,2], J.R. Kimmel[1], A. Trimborn[4], J. Jayne[4], A. C. Aiken[1,3], M. Gonin[5], K. Fuhrer[5], T. Horvath[5], K.S. Docherty[1], D.R. Worsnop[4], and J.L. Jimenez[1,3,*]

[1]Cooperative Institute for Research in the Environmental Sciences (CIRES), University of Colorado at Boulder
[2]Department of Atmospheric and Oceanic Science, University of Colorado at Boulder
[3]Department of Chemistry and Biochemistry, University of Colorado at Boulder
[4]Aerodyne Research Incorporated, Billerica MA
[5]Tofwerk AG, Thun, Switzerland

Table of Contents:

Table S-1. Typical HR-ToF-AMS data acquisition parameters for V and W modes, for m/z ranges up to 300 and 500 amu. The minimum *m/z* sampled is determined by the trigger delay and for these settings is approximately 10 amu.

Acquisition Parameter	V-Mode (300)	V-Mode (500)	W-Mode (300)	W-Mode (500)
Pulser Period (μs)	28	35	56	72
Nbr of Spectra per chopper cycle	160	140	80	70
Nbr of Samples	23488	30688	46976	61984
Nbr of Co-adds	1	1	1	1
Nbr of Chopper Cycles co-averaged	300	300	300	300
Chopper Frequency (Hz)	160	160	160	160
Acqusition Trigger Delay (ns)	4000	4000	9000	9000
Data Delay for PToF (μs)	200	200	200	200

Figure S-1. Spectra of PFK in both V and W modes of the HR-ToF-AMS. Note the *m/z* axis difference. The V-Mode data show detectable signal up to *m/z* 1300, whereas the W-mode's lower sensitivity results in detectable signal up to only *m/z* 700.

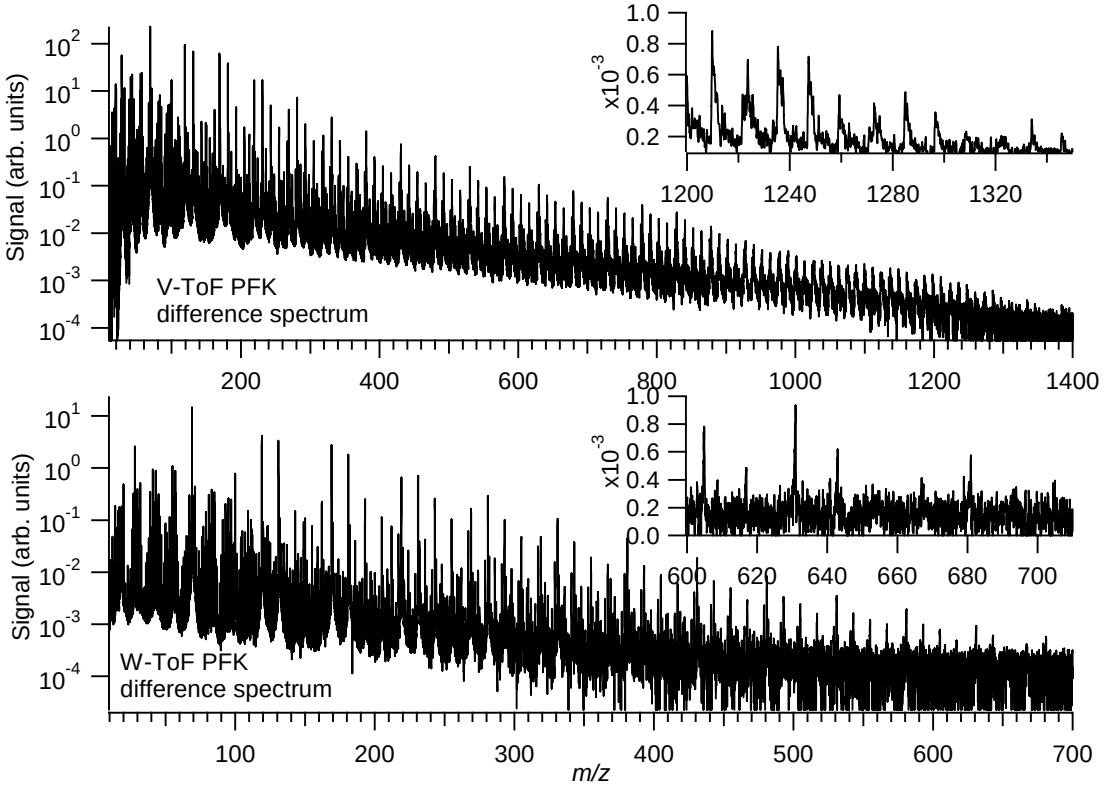

Figure S-2. Peak Width (σ) as a function of *m/z* for W-Mode HR-ToF-AMS Data from the SOAR-1 field experiment. The results of a linear Regression are also shown.

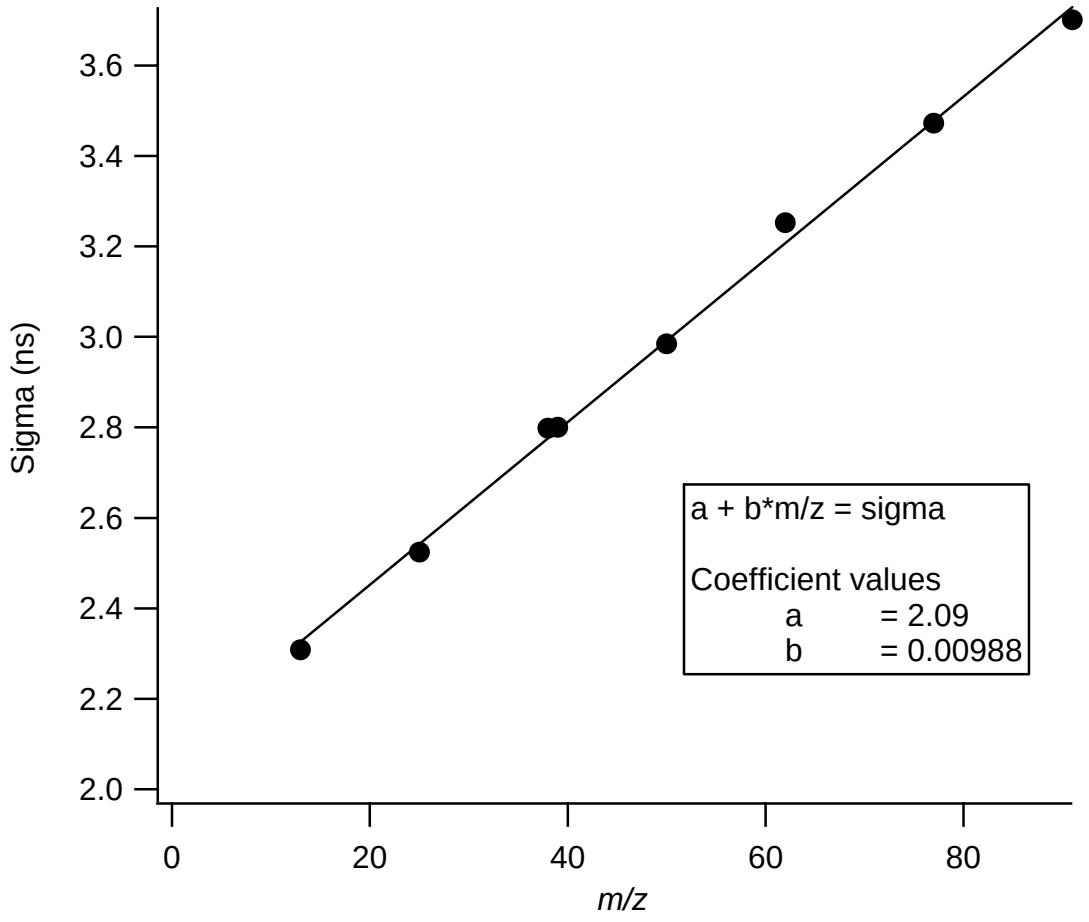

Figure S-3. Peak shape function in black as determined by isolated ion shapes. Colored dots correspond to data from different *m/z* ions. The black line through the data is the peak shape function used in the peak fitting algorithm. The green curve denotes a true Gaussian shape, and the blue curve is the Gaussian curve multiplied by the peak shape function, giving the "true" ion peak shape.